Lawrence Berkeley National Laboratory
Recent Work

Title
Seismic detection of fault and fracture systems

Permalink
https://escholarship.org/uc/item/7vq866m9

Author
Majer, Ernest L.

Publication Date
2004-01-20

Seismic Detection of Fault and Fracture Systems

Roland Gritto and Ernest L. Majer
Lawrence Berkeley National Laboratory
One Cyclotron Road
Berkeley, California 94720

ABSTRACT

A finite-difference modeling study of seismic wave propagation was conducted to determine how to best investigate subsurface faults and fracture zones in geothermal areas. The numerical model was created based on results from a previous seismic reflection field experiment. A suite of fault models was investigated including blind faults and faults with surface expressions. The seismic data suggest that blind faults can be detected by a sudden attenuation of seismic wave amplitudes, as long as the fault is located below the receiver array. Additionally, a conversion from P- to S-waves indicates the reflection and refraction of the P-waves while propagating across the fault. The drop in amplitudes and the excitation of S-waves can be used to estimate the location of the fault at depth. The accuracy of the numerical modeling depends on the availability of a priori in situ information (velocity and density) from borehole experiments in the geothermal area.

Keywords: 2-D Seismic FD Modeling, Seismic-Wave-Interaction with Faults and Fractures

Introduction

The geothermal energy potential in the western United States is vast, but at present the cost of geothermal heat and electricity remains higher than most conventional energy technologies. To expand the resource base the efficiency of known geothermal areas the Department of Energy has established an Enhanced Geothermal Systems Program (EGSP) to understand and demonstrate the technology to produce electric power from artificially created geothermal systems. The challenges in developing Enhanced Geothermal Systems (EGS) include, among others factors, the location of stressed fracture systems with increased permeability and adequate water supply. The characteristics of these fracture systems that need to be determined include the orientation, size, extent, permeability, and state of stress. Furthermore, it is necessary to distinguish between permeable pathways and porous but less-permeable zones.

Seismic imaging methods have been successfully used in the oil and gas industry to detect and characterize fractured gas- and oil reservoirs, but these surveys have mostly been used in sedimentary basins where the stratigraphy often consists of horizontal layering. In contrast, the extreme heterogeneity, anisotropy, and mixed fluid phases found in many geothermal areas pose a significant challenge for conventional seismic

imaging techniques. Therefore, an extension and adaptation of current methods is needed to optimize state-of-the-art multi-component 3-D and 4-D imaging methods for geothermal applications.

In the current paper, we perform finite difference (FD) modeling of seismic wave propagation in geothermal areas with realistic physical properties to characterize seismic wave interaction with faults and fracture systems typical for EGS.

Faults, Fracture Systems, and Seismic Waves

It is widely accepted that an increase in water circulation is needed to improve the efficiency of geothermal systems. Discrete faults with increased permeability present pathways for an increase in water flow. Similarly, zones of increased fracturing may constitute flow paths with even higher permeability depending on the fracture density. It is therefore desirable to detect and map faults and fracture zones and characterize their physical properties. Surface and borehole seismic imaging methods can generally be used to estimate these properties, but further development is needed for the application in geothermal areas.

Seismic wave propagation in a homogeneously layered velocity model can lead to complicated wave fields even in the absence of structural features like faults or fracture zones. If these features are present, however, the seismic wave field becomes much more complicated and the seismic "foot print" of the fault/fracture zones may be masked and difficult to observe. Therefore, it is important to study the characteristics of seismic wave interaction with faults and fracture zones to establish typical patterns that can be recognized in seismic field data. General questions to investigate include the depth extent of faults. Is the seismic signature of blind faults (i.e., the fault plane doesn't break the surface) different from faults extending all the way to the surface? How can faults be distinguished from zones of high fracturing? Other parameters include the strike and dip as well as width of the fault or fracture zone. The fracture stiffness may be estimated from seismic waves, which could yield such important parameters as contact area or degree of mineralization within a fault or fracture. Numerical modeling of seismic wave interaction with faults and fracture zones is an important tool to investigate the physics of the problem and to develop new imaging methods to be applicable to geothermal areas.

Finite-Difference Modeling

Finite-difference modeling (Nihei et al., 2002) was used to simulate seismic wave propagation in a geothermal area with a layered velocity structure in the presence of different types of faults. The velocity model was taken from previous borehole studies at the Rye Patch geothermal reservoir (Gritto et al., 2003). The P- and S-wave velocity models are shown in Figure 1. The parameters of the fault were modeled after Coates and Schoenberg (1995), where the orientation of the fault relative to the finite-difference grid and the fault stiffness are translated into elastic constants using equivalent medium

theory. The central frequency of the source wavelet was 25 Hz to simulate the frequency content of the source wavelet used in the field case. The source and receiver positions are taken from a 3-D seismic reflection survey conducted at Rye Patch in 1998 (Feighner et al., 1999). The vertical line below the receiver array in Figure 1 indicates the location of the fault and is based on results by Teplow (1999). It is modeled as a blind fault (terminated below the surface) representing the situation in the field. The fault in the current model was chosen to represent a weak structure with low isotropic stiffness or high compliance (λ=2.92 GPa, μ=10.89 GPa, ρ=2.5 g/cm^3) and a fault width of 18 m (i.e., in the shallow parts of the velocity model the wavelengths of the P- and S-waves are, respectively, 6 and 3.5 times larger than the fault width).
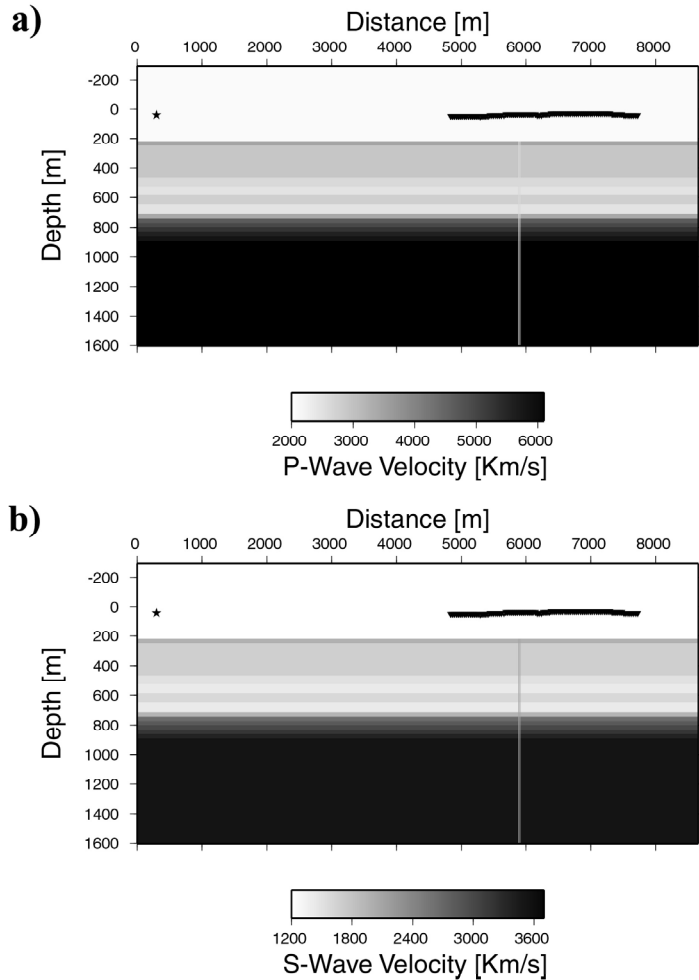

Figure 1: 2-D velocity model used for the numerical modeling study. The model is based on VSP data taken at the Rye Patch geothermal reservoir (Gritto et al, 2003). The star denotes the seismic source (isotropic velocity displacement), while the triangles indicate a receiver array. The location of the fault is show by a vertical line terminating at 200 m depth below the receiver array. (a) P-wave velocity model. (b) S-wave velocity model.

Results

The results of one FD simulation are shown in Figure 2. They represent four snap shots in time of the seismic wave fields (vertical particle-velocity) propagating from the source through the subsurface to the receiver array. The times shown along the right margin represent the travel time for each frame. The snap shots indicate the complicated nature of the seismic wave field even for this relatively simple model of a homogeneously layered medium. The wave front, arriving at the receiver array first, belongs to P-waves that were refracted along the high velocity basement (see Figure 1a). Behind the initial P-

waves an interference pattern of reflected and refracted P- and S-waves (generated by P-to-S conversion at the first interface) is visible (see first panel T=1.25 s). At time T=1.4 s the initial P-waves interfere with the tip of the fault and their energy is scattered in the process (elastic scattering). It can be seen that the amplitude of the wave front is reduced behind the fault tip. In the next time frame (T=1.5 s), the P-waves have passed the fault and converted S-waves are visible propagating upwards along the fault trace. The last frame, at T=1.8s, shows that the P-waves have reached the end of the receivers, while the converted S-waves are still propagating across the array. It is evident that the amplitudes of the P-waves have healed along the wave front during their propagation away from the fault. It should be noted that the model in Figure 1 contained boundary conditions that prevented the reflection of energy from the margins of the model. The absorbing conditions were also applied to the surface of the model to suppress surface waves and reflections (multiples) between the free surface and the subsurface interfaces. The surface waves would not have interfered with the wave fronts shown in Figure 2, because they would have reached the receiver array at times later than T=4.0 s. The seismic energy reflected between the free surface and the subsurface interfaces, however, would have coincided with the waves presented above and was suppressed to concentrate on the pattern of seismic energy created by the fault alone. The case of a free surface will be included in the results presented at the 2003 GRC meeting.

Figure 2: Time snap shots (vertical particle-velocity) of wave field propagation across the model show in Figure 1. The representative time for each snap shot is indicated to the right of each frame.

The seismograms recorded along the receiver array should reflect the kinematics observed in the snapshots in Figure 2. These seismograms are presented in Figure 3, where the amplitudes are trace normalized to emphasize the presence of each phase. The first arriving P-wave can be seen across the receiver array, with a gap between receivers 51 and 61, indicating the attenuation caused by the presence of the fault. The S-waves that reflect and refract off the fault, as previously seen in the time snap shots, are evident as amplitudes originating from the gap in the seismograms. Later arrivals indicate a combination of reflected and refracted P- and S- waves from layers above the basement. The numerical results indicate that the presence of the fault below the receiver array is evident by the gap in continuity of P-wave amplitudes coupled with the excitation of S-waves through P-wave interaction with the fault. A comparison of the numerical results to field data could determine whether similar effects can be expected in geothermal field settings.
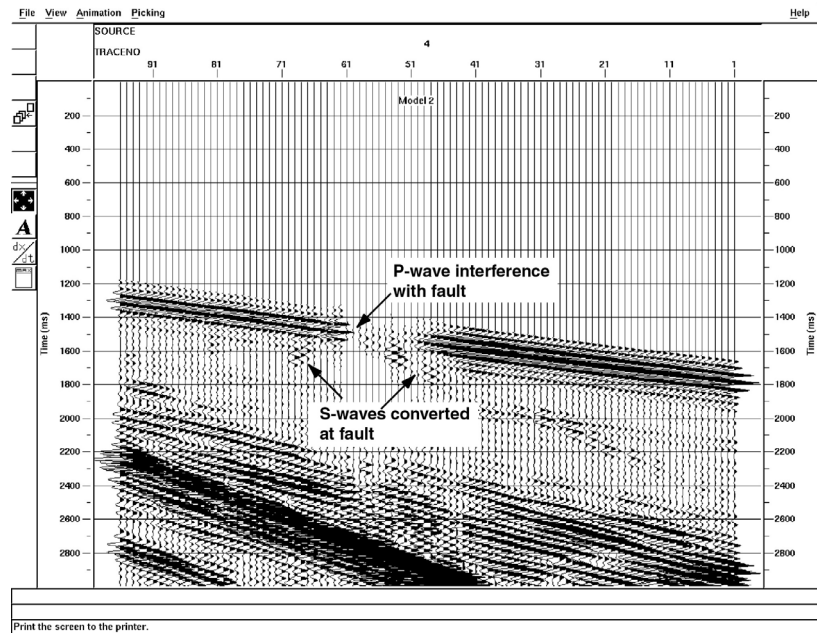

Figure 3: Numerical seismogram section of the vertical particle-velocity representing the seismic waves recorded by the receiver array shown in Figures 1 and 2. Note the sudden attenuation of the first arriving P-waves between traces 51 and 61.

As mentioned before, the numerical model above was derived from the field geometry of one source-receiver line during the 1998 seismic reflection survey at Rye Patch (Feighner et al., 1999), which ran across the location of a postulated blind fault at depth. The seismic field data recorded by the receiver array is presented in Figure 4. It can be seen that, to first order, effects, similar to the ones described in the numerical results, can be observed. The amplitudes of the first arriving P-waves exhibit a similar move out and arrival times on the seismograms as in the numerical study. Furthermore, the amplitudes reveal a sudden drop around the location of receiver number 61. Although the recovery of the wave front is not as apparent as before, this effect is still noticeable by coherent arrivals at later times bounded by the solid lines between receiver numbers 21 and 31. The poor signal-to-noise ratio of the field data, however, masks any converted S-waves generated by interaction of the P-waves with the fault. Additionally to the elastic scattering by the fault, the subsurface at Rye Patch exhibits a considerable amount of heterogeneity and anelastic attenuation that are not taken into account in the numerical simulations above. Nevertheless, the similarities between the numerical and field data are

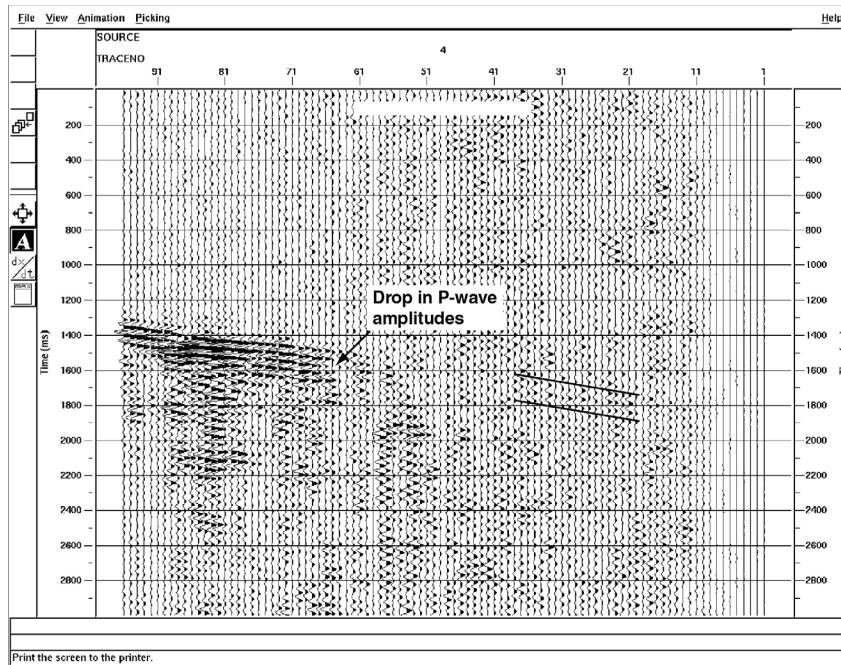intriguing and help us to understand seismic wave interaction with subsurface faults in heterogeneous media.

Figure 4: Seismic field data (vertical particle-velocity) recorded at Rye Patch along the actual receiver array modeled in Figures 1 and 2. Notice the abrupt change in amplitudes of the first arrivals, as indicated by the arrow. At later times, amplitudes recover marginally, as indicated by the coherent phases between receiver position 21 and 31.

Conclusions

Numerical modeling of seismic wave propagation in geothermal areas provides a tool to study the effect of heterogeneity and structural unconformities on the results of seismic field studies before the experiment is conducted. Thus, it is possible to predict certain results and optimize the survey design to maximize success. The numerical models, however, need to be comprised of realistic parameters, which require a priori information from vertical seismic profiling (VSP) or logging data.

The results of the numerical study thus far can be summarized as follows.

- If a blind fault is expected to be present in the subsurface, the receiver array should be placed in close proximity, possibly directly above the assumed location, to detect the observed attenuation of the P-waves by the fault tip, because wave front healing may mask this effect for receivers at far offsets from the fault.
- If a receiver array is located above a vertical fault, P-waves propagating across this fault will generate refracted and reflected P- and S-waves that reveal an apex around the location of the fault tip.

6

In our presentation, we will present results of 2-D and 3-D seismic reflection surveys and show the strength and limitations of these methods to resolve parameters of fault and fracture zones in realistic geological settings.

Acknowledgments

References

Coates, R.T., and Schoenberg, M., 1995, Finite-difference modeling of faults and fractures, Geophysics, Vol. 60, No. 5, pp. 1,514-1,526.

Feighner, M., Gritto, R., Daley, T.M., Keers, H., and Majer, E.L., 1999, Three-Dimensional Seismic Imaging of the Rye Patch Geothermal Reservoir, Lawrence Berkeley National Laboratory Report LBNL-44119.

Gritto, R., Daley, T.M., and Majer, E.L., 2003, Estimating subsurface topography from surface-to-borehole seismic studies at the Rye Patch geothermal reservoir, Nevada, USA, Geothermics, Vol. 32, No. 3, LBNL-50490.

Nihei, K.T., Nakagawa, S., Myer, L.R., and Majer, E.L., 2002, Finite difference modeling of seismic wave interactions with discrete, finite length fractures, Proceedings Seventy-Second Annual Meeting, Society of Exploration Geophysicist, Salt Lake City, USA.

Teplow, B., 1999. Integrated Geophysical Exploration Program at the Rye Patch Geothermal Field, Pershing County, Nevada, Final Report to Mount Wheeler Power.